

# A New Li–Al–N–H System for Reversible Hydrogen Storage

Jun Lu, Zhigang Zak Fang,\* and Hong Yong Sohn

Department of Metallurgical Engineering, University of Utah, 135 South 1460 East Room 412, Salt Lake City, Utah 84112

Received: March 21, 2006; In Final Form: May 25, 2006

Complex metal hydrides are considered as a class of candidate materials for hydrogen storage. Lithium-based complex hydrides including lithium alanates ( $\text{LiAlH}_4$  and  $\text{Li}_3\text{AlH}_6$ ) are among the most promising materials owing to its high hydrogen content. In the present work, we investigated dehydrogenation/rehydrogenation reactions of a combined system of  $\text{Li}_3\text{AlH}_6$  and  $\text{LiNH}_2$ . Thermogravimetric analysis (TGA) of  $\text{Li}_3\text{AlH}_6/3\text{LiNH}_2/4 \text{ wt } \% \text{ TiCl}_3\text{--}1/3\text{AlCl}_3$  mixtures indicated that a large amount of hydrogen ( $\sim 7.1 \text{ wt } \%$ ) can be released between  $150^\circ\text{C}$  and  $300^\circ\text{C}$  under a heating rate of  $5^\circ\text{C}/\text{min}$  in two dehydrogenation reaction steps. The results also show that the dehydrogenation reaction of the new material system is nearly 100% reversible under 2000 psi pressure hydrogen at  $300^\circ\text{C}$ . Further, a short-cycle experiment has demonstrated that the new combined material system of alanates and amides can maintain its hydrogen storage capacity upon cycling of the dehydrogenation/rehydrogenation reactions.

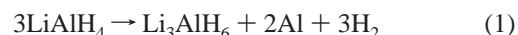
## 1. Introduction

The demand for efficient and clean fuel alternatives has increased in recent years and is expected to become more pronounced in the future.<sup>1,2</sup> Hydrogen is viewed as the most promising clean fuel of the future because of its abundance, easy synthesis, and nonpolluting nature when burned.<sup>3–5</sup> However, the development of hydrogen as a major energy carrier will require solutions to many scientific and technological challenges. Foremost among these is the issue of hydrogen storage. Although hydrogen gas ( $\text{H}_2$ ) has an excellent energy content per unit weight, it has low energy content per unit volume. Therefore, the development of an alternative hydrogen storage technology is of critical importance.

Metal hydrides are considered as a promising class of materials for hydrogen storage because they store hydrogen in a safe and efficient way while having volumetric densities comparable to or greater than liquid hydrogen. Following the breakthrough work on Ti-doped  $\text{NaAlH}_4$  by Bogdanovic and Schwickardi in 1997,<sup>6</sup> lithium alanates ( $\text{LiAlH}_4$ ) as well as alanates of other alkali- and alkaline-earth-metal-based complex aluminum hydrides have received a great deal of attention as possible candidate materials because of their lightweight and high inherent storage capacity.<sup>7–20</sup> However, it has generally been found that the dehydrogenation reaction of  $\text{LiAlH}_4$  is not easily reversible, which is a critical requirement for on-board hydrogen storage applications.<sup>7–11</sup> In addition, one of the reaction steps during the complete dehydrogenation of  $\text{LiAlH}_4$  is the decomposition of  $\text{LiH}$  that requires temperatures higher than  $700^\circ\text{C}$ , which is also unacceptable for practical vehicular applications.<sup>21</sup>

One approach for improving the performance of monolithic metal hydrides is through the combination and reactions among metal hydrides. In an effort to study the potential of lithium-based materials, Chen et al.<sup>22,23</sup> and Hu et al.<sup>24–26</sup> reported that the dehydrogenation temperature of  $\text{LiH}$  could be decreased

dramatically when it is combined with  $\text{LiNH}_2$ . Recently, Lu and Fang<sup>27</sup> discovered that if  $\text{LiAlH}_4$  and  $\text{LiNH}_2$  are combined, the  $\text{LiH}$  that forms as an intermediate product of the dehydrogenation of  $\text{LiAlH}_4$  can react with  $\text{LiNH}_2$  to release  $\text{H}_2$  at low temperatures. The reactions steps and the overall reactions are given in eqs 1–4:



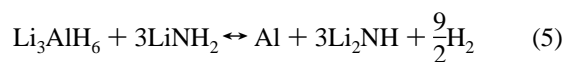
In other words, all the hydrogen contained in  $\text{LiAlH}_4$  can be released, which raises the effective hydrogen storage capacity of  $\text{LiAlH}_4$  to nearly 10 wt %.

However, the reversibility of the above reactions remains a major technical hurdle even when the combination approach is employed. In an attempt to demonstrate the reversibility of reaction 4, Lu and Fang<sup>28</sup> were able to demonstrate only 3.5–4.0 wt % hydrogen to be reversible from  $100^\circ\text{C}$  to  $380^\circ\text{C}$  under 2000 psi hydrogen pressure, which is less than 50% of the hydrogen in the original sample of  $\text{LiAlH}_4 + \text{LiNH}_2$ . The difficulty of reversing reaction 4 is attributed to the irreversibility of reaction 1.<sup>8,29–32</sup> Using CALPHAD thermodynamic modeling tool, Jang et al.<sup>32</sup> found that the reaction from  $\text{Li}_3\text{AlH}_6$  (lithium hex aluminum hydride) to  $\text{LiAlH}_4$  ( $\text{Li}_3\text{AlH}_6 + 3\text{H}_2 + 2\text{Al} = 3\text{LiAlH}_4$ ) is thermodynamically difficult within the temperature and pressure ranges in which the studies were carried out, which was confirmed by Zaluski et al.<sup>29</sup> and Balema et al.<sup>30,31</sup> using differential thermal analysis (DTA). On the other hand, however, the results of Jang et al.<sup>32</sup> do show that the reaction  $3\text{LiH} + \text{Al} + \frac{3}{2}\text{H}_2 = \text{Li}_3\text{AlH}_6$  is thermodynamically feasible.

On the basis of the above information, it is hypothesized that if  $\text{Li}_3\text{AlH}_6$  and  $\text{LiNH}_2$  are combined in a proper ratio, the

\* Author to whom correspondence should be addressed. Tel: (801) 581-8128; fax: (801) 581-4937; e-mail: zfang@mines.utah.edu.

dehydrogenation reactions of the combined system could be reversible. The overall reaction equation of a combined  $\text{Li}_3\text{AlH}_6/3\text{LiNH}_2$  system would be given by



Similar to the combination of  $\text{LiAlH}_4$  and  $\text{LiNH}_2$ , the  $\text{LiH}$  that forms as an intermediate product of the decomposition of  $\text{Li}_3\text{AlH}_6$  on the basis of reaction 2 can react with  $\text{LiNH}_2$  according to reaction 3 to release  $\text{H}_2$  at a lower temperature. In effect, all the hydrogen contained in  $\text{Li}_3\text{AlH}_6$  is released by the overall reaction 5.

In the present work, the new combined system ( $\text{Li}_3\text{AlH}_6/3\text{LiNH}_2$ ), which has a very high theoretical hydrogen capacity, 7.3 wt % according to reaction 5, is studied. As it will become clear through the results described hereafter, the dehydrogenation of lithium hex aluminum hydride via its reaction with lithium amide is reversible, while the dehydrogenation of lithium alanate via its reaction with lithium amide, as reported in ref 27, is not. The following experimental results will show dehydrogenation and rehydrogenation behaviors of this new material system. The reaction paths and mechanisms of the combined system will also be discussed.

## 2. Experimental Section

The starting materials, lithium aluminum hydride ( $\text{LiAlH}_4$ , 95%), lithium hydride ( $\text{LiH}$ , 95%), lithium amide ( $\text{LiNH}_2$ , 95%), aluminum powder ( $\text{Al}$ , 99%), and  $\text{TiCl}_3\text{--}\frac{1}{3}\text{AlCl}_3$ , were purchased from Aldrich Chemicals and were used as received without any further purification. The  $\text{Li}_2\text{NH}$  sample was prepared by decomposing commercial  $\text{LiNH}_2$  at temperatures above 450 °C in argon atmosphere.  $\text{Li}_3\text{AlH}_6$  was synthesized by reacting  $\text{LiH}$  with  $\text{LiAlH}_4$  in a ball mill. To prevent samples and raw materials from undergoing oxidation or hydroxide formation, they were stored and handled in an argon-filled glovebox. Reactant mixtures were prepared using mechanical milling. Approximately 1.0 g mixtures were milled using a Spex 8000 mill under argon atmosphere.  $\text{TiCl}_3\text{--}\frac{1}{3}\text{AlCl}_3$  was added as a catalyst for a rehydrogenation reaction.<sup>8</sup>

The thermal dehydrogenation properties of the mixture ( $\text{Li}_3\text{AlH}_6/3\text{LiNH}_2/4$  wt %  $\text{TiCl}_3\text{--}\frac{1}{3}\text{AlCl}_3$ , sample 1) were determined by the use of a thermogravimetric analyzer (TGA) (Shimadzu TGA50) upon heating to 350 °C at a heating rate of 5 °C/min, which is also conducted inside the argon-filled glovebox. The rehydrogenation of the mixture ( $\text{Al}/3\text{Li}_2\text{NH}/4$  wt %  $\text{TiCl}_3\text{--}\frac{1}{3}\text{AlCl}_3$ , sample 2) was performed by using a custom-made autoclave with a hydrogen pressure limit of 5000 psi at 500 °C. The rehydrogenation experiments were conducted by heating 500 mg of the above mixture to 300 °C at a heating rate of 5 °C/min and by holding at 300 °C for 1–4 h under 2000 psi of hydrogen. Cycling experiments of sample 2 were performed by using the same procedures for dehydrogenation and rehydrogenation as described above. Samples after six cycles were analyzed using TGA.

The identification of reactants and reaction products in the mixture before and after the TGA runs was carried out using a Siemens D5000 model X-ray diffractometer with Ni-filtered  $\text{Cu K}\alpha$  radiation ( $\lambda = 1.5406$  Å). A scanning rate of 0.02°/s was applied to record the patterns in the  $2\theta$  range of 10–90°. An amorphous-like background in the XRD patterns exists in the patterns of all samples. It is attributed to the thin plastic films that were used to cover the powders and is subtracted from the patterns presented in the following results.

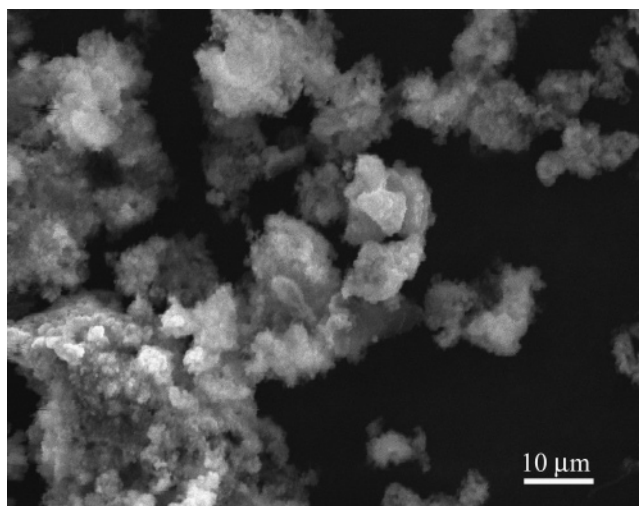


Figure 1. SEM micrographs of sample 1 after Spex mill.

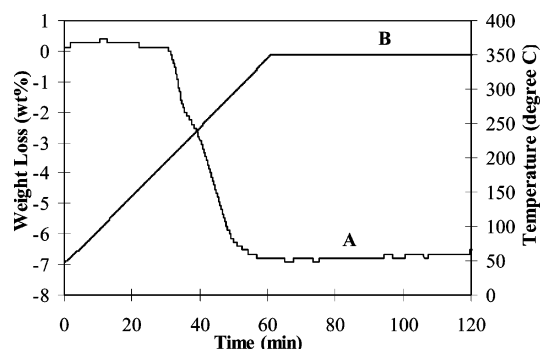


Figure 2. TGA curves for sample 1. Curve (A) shows the hydrogen generation from the  $\text{Li}_3\text{AlH}_6/3\text{LiNH}_2/4$  wt %  $\text{TiCl}_3\text{--}\frac{1}{3}\text{AlCl}_3$  system under argon atmosphere and a heating rate of 5 °C/min. Curve (B) shows the temperature profile.

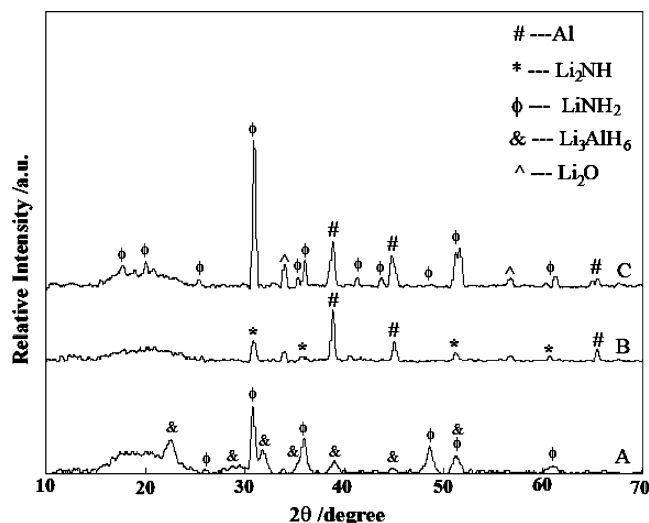
A scanning electron microscope (SEM) was used to characterize the particle size and morphology of the sample after milling. SEM samples were prepared by attaching a small amount of the milled powders in a conductive tape in the glovebox. Figure 1 shows a typical SEM image of sample 1 after Spex mill. It shows that the particles were aggregated and that the size of the aggregated particles is approximately 2–10  $\mu\text{m}$ .

## 3. Results and Discussion

### 3.1. Dehydrogenation of $\text{Li}_3\text{AlH}_6/3\text{LiNH}_2/4$ wt % $\text{TiCl}_3\text{--}\frac{1}{3}\text{AlCl}_3$ .

Figure 2 shows the TGA result of the  $\text{Li}_3\text{AlH}_6/3\text{LiNH}_2/4$  wt %  $\text{TiCl}_3\text{--}\frac{1}{3}\text{AlCl}_3$  (sample 1). The experiment was run under argon atmosphere with a heating rate of 5 °C/min. Each reaction step is identified by the changes in the weight loss rate. It can be seen that a total 7.1 wt % of hydrogen was released within the temperature range tested. The dehydrogenation process appears to consist of two steps: The first step is in the temperature range of 160–200 °C. A total of 2.4 wt % of hydrogen was released by this step, which can best be described by reaction 2. The second step occurs at above 210 °C. Another 4.7 wt % hydrogen was released during the second step, which corresponds to reaction 3. The overall dehydrogenation reaction, which is a combination of reaction 2 and reaction 3, is given by reaction 5. The total 7.1 wt % of weight loss as shown in Figure 2 indicates that the dehydrogenation is complete.

To verify these specific reaction steps, X-ray diffraction was used to analyze both the raw materials and the reaction products.



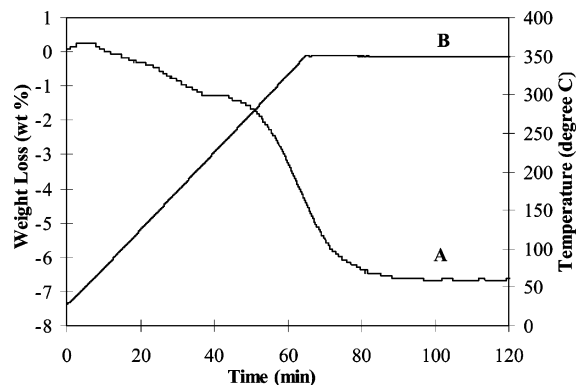
**Figure 3.** XRD patterns of (A) sample 1 after ball milling, (B) sample 1 after being heated to 300 °C, and (C) sample 1 after being heated to 200 °C.

Figure 3 shows the XRD patterns of selected samples before and after dehydrogenation. Crystalline phases are identified by comparing the experimental data with JCPDS (Joint Committee on Powder Diffraction Standards) files from the International Center for Diffraction Data. In Figure 3A, which shows the XRD pattern of sample 1 before dehydrogenation, the peaks marked with “&” are attributed to the  $\text{Li}_3\text{AlH}_6$  phase and those marked with “φ” are attributed to the tetragonal  $\text{LiNH}_2$  phase. No characteristic peaks of crystalline  $\text{TiCl}_3\text{--}\frac{1}{3}\text{AlCl}_3$  are observed, which is attributed to their low contents. Figure 3B shows the XRD patterns of sample 1 after dehydrogenation. The XRD patterns clearly show that  $\text{Li}_3\text{AlH}_6$  and  $\text{LiNH}_2$  are absent in the samples, indicating that they are consumed by the decomposition and reactions. The patterns do show new compounds formed. In these figures, the peaks that are marked with an asterisk are indexed to be the cubic phase of  $\text{Li}_2\text{NH}$  and those marked with # are indexed to be Al or Al + LiH (Al and LiH peaks overlap on the XRD patterns.) However, these peaks could only be those of Al in this case because when the hydrogenation reaction 3 is complete, all LiH is consumed.

Figure 3 confirms the overall dehydrogenation reaction 5 by identification of the final reaction products. However, it does not provide any information regarding the reaction path. To determine the reaction paths, that is, the intermediate reactions, two approaches were taken. First, reaction 2 and reaction 3 are proposed as the intermediate reactions because the molar balance of these reactions matches with the weight loss steps present in the TGA curve in Figure 2. To further confirm each reaction step, the intermediate products after partial dehydrogenation at specific temperatures were analyzed using XRD. Figure 3C shows the XRD pattern of the product after dehydrogenation at 200 °C for 30 min, in which the peaks that are marked with # are indexed to be cubic aluminum and LiH and those marked with “φ” are indexed to be tetragonal  $\text{LiNH}_2$ . This confirms that the first dehydrogenation step corresponds to reaction 2.

### 3.2. Rehydrogenation of $\text{Al}/3\text{Li}_2\text{NH}/4 \text{ wt } \% \text{ TiCl}_3$ .

To study the reversibility of the combined  $\text{Li}_3\text{AlH}_6/3\text{LiNH}_2$  system, the rehydrogenation of sample 2 ( $\text{Al}/3\text{Li}_2\text{NH}/4 \text{ wt } \% \text{ TiCl}_3\text{--}\frac{1}{3}\text{AlCl}_3$ ), which is the dehydrogenated products of sample 1, was carried out by using a custom-made autoclave under 2000 psi  $\text{H}_2$  pressure and at 300 °C. Figure 4 shows TGA curves of the hydrogenated sample 2. It shows that sample 2 gained about 7.0 wt % hydrogen from the rehydrogenation



**Figure 4.** TGA curves for sample 2 after hydrogenation. Curve (A) shows the hydrogen generation under argon atmosphere and a heating rate of 5 °C/min. Curve (B) shows the temperature profile.

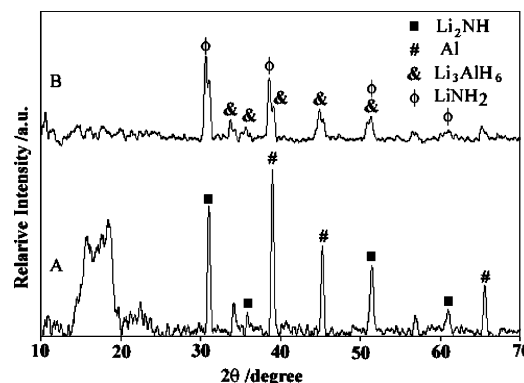


**Figure 5.** XRD patterns of (A) sample 2 after ball milling and (B) sample 2 after rehydrogenation.

process. The TGA curve shows two dehydrogenation steps of the hydrogenated sample 2, which is nearly identical to the original dehydrogenation curve of sample 1. This demonstrates that the hydrogenation of sample 2 is complete. In other words, the dehydrogenation of  $\text{Li}_3\text{AlH}_6/3\text{LiNH}_2$  is reversed.

To further verify the reaction paths, X-ray diffraction analysis was carried out on sample 2 before and after hydrogenation. In Figure 5A, which shows the XRD pattern of sample 2 before hydrogenation, the peaks marked with # are attributed to the phase of Al and those marked with closed squares are attributed to the phase of  $\text{Li}_2\text{NH}$ . Figure 5B shows the XRD patterns of sample 2 after hydrogenation. The XRD patterns clearly show that Al and  $\text{Li}_2\text{NH}$  are absent in the sample, indicating that they are consumed by reaction with hydrogen and that some new compounds formed. In this figure, the peaks that are marked with “&” are indexed to be the cubic phase of  $\text{Li}_3\text{AlH}_6$  and those marked with “φ” are indexed to be  $\text{LiNH}_2$ . No other phases were present. Once again, the XRD results confirm that sample 2 was completely hydrogenated and that reaction 5 is reversible.

To further demonstrate the reversibility of reaction 5, short cyclic experiments of the dehydrogenation and rehydrogenation reactions were carried out using the autoclave system as described earlier. Selected specimens of sample 1 were placed in the reaction vessel and were subjected to dehydrogenation and rehydrogenation procedures as described for samples 1 and 2. Six cycles of dehydrogenation and rehydrogenation were carried out. The specimens after the cyclic experiments were then analyzed using TGA. The results are shown in Figure 6, which demonstrates that the material maintains 6.9 wt % hydrogen storage capacity after the short-cycle experiment.

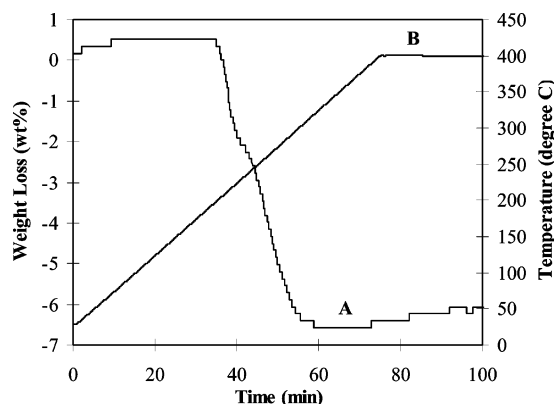


**Figure 6.** TGA curves for sample 2 after six hydrogenation/dehydrogenation cycles. Curve (A) shows the hydrogen generation under argon atmosphere and a heating rate of 5 °C/min. Curve (B) shows the temperature profile.

#### 4. Conclusions

The dehydrogenation and rehydrogenation reactions of a combined system of lithium hex aluminum hydride and lithium amide were investigated. Thermogravimetric analysis (TGA) of the  $\text{Li}_3\text{AlH}_6/3\text{LiNH}_2/4 \text{ wt } \% \text{ TiCl}_3\text{--}1/3\text{AlCl}_3$  mixture indicated that a total of 7.1 wt % hydrogen can be released between 150 °C and 300 °C under a heating rate of 5 °C/min in two dehydrogenation reaction steps. The rehydrogenation experiment of the dehydrogenated sample proved that the dehydrogenation reaction of the combined  $\text{Li}_3\text{AlH}_6/3\text{LiNH}_2$  system is nearly 100% reversible. The results of the short-cycle experiments further demonstrated that the new material system could maintain its hydrogen storage capacity upon cycling of the dehydrogenation and rehydrogenation reactions.

**Acknowledgment.** This research was made possible by the financial support from the U.S. Department of Energy (DOE) under contract number DE-FC36-05GO15069 since March 2005. The work was conducted as a part of the project within the Metal Hydride Center of Excellence led by the Sandia National Laboratory, which is also funded by the U.S. Department of Energy.

#### References and Notes

(1) Elam, C. C.; Padr, C. E. G.; Sandroock, G.; Luzzi, A.; Lindblad, P.; Hagen, E. F. *Int. J. Hydrogen Energy* **2003**, *28*, 601.

- (2) Conte, M.; Iacobazzi, A.; Ronchetti, M.; Vellone, R. *J. Power Sources* **2001**, *100*, 171.
- (3) Dell, R. M.; Rand, D. A. J. *J. Power Sources* **2001**, *100*, 2.
- (4) McNicol, B. D.; Rand, D. A. J.; Williams, K. R. *J. Power Sources* **2001**, *100*, 47.
- (5) Stambouli, A. B.; Traversa, E. *Renewable Sustainable Energy Rev.* **2002**, *6*, 297.
- (6) Bogdanovic, B.; Schwickardi, M. *J. Alloys Compd.* **1997**, *253*, 1.
- (7) Balema, V. P.; Dennis, K. W.; Pecharsky, V. K. *Chem. Commun.* **2000**, *17*, 1665.
- (8) Chen, J.; Kuriyama, N.; Xu, Q.; Takeshita, H. T.; Sakai, T. *J. Phys. Chem. B* **2001**, *105*, 11214.
- (9) Blanchard, D.; Brinks, H. W.; Hauback, B. C.; Norby, P. *Mater. Sci. Eng., B* **2004**, *108*, 54.
- (10) Brinks, H. W.; Hauback, B. C.; Norby, P.; Fjellvåg, H. *J. Alloys Compd.* **2003**, *351*, 222.
- (11) Hauback, B. C.; Brinks, H. W.; Fjellvåg, H. *J. Alloys Compd.* **2002**, *346*, 184.
- (12) Zidan, R. A.; Taraka, S.; Hee, A. G.; Jensen, C. M. *J. Alloys Compd.* **1999**, *285*, 119.
- (13) Zaluska, A.; Zaluski, L.; Strom-Olsen, J. O. *J. Alloys Compd.* **2000**, *298*, 125.
- (14) Bogdanovic, B.; Schwickardi, M. *Appl. Phys. A* **2001**, *72*, 221.
- (15) Jensen, C. M.; Gross, K. J. *Appl. Phys. A* **2001**, *72*, 213.
- (16) Sandroock, G.; Gross, K. J.; Thomas, G. *J. Alloys Compd.* **2002**, *339*, 299.
- (17) Sun, D. L.; Kiyobayashi, T.; Takeshita, H. T.; Kuriyama, N.; Jensen, C. M. *J. Alloys Compd.* **2002**, *337*, 8.
- (18) Kiyobayashi, T.; Srinivasan, S.; Sun, D. L.; Jensen, C. M. *J. Phys. Chem. A* **2003**, *107*, 7671.
- (19) Brinks, H. W.; Jensen, C. M.; Srinivasan, S. S.; Hauback, B. C.; Blanchard, D.; Murphy, K. *J. Alloys Compd.* **2004**, *376*, 215.
- (20) Morioka, H.; Kakizaki, K.; Chung, S. C.; Yamada, A. *J. Alloys Compd.* **2003**, *353*, 310.
- (21) Grochala, W.; Edwards, P. *Chem. Rev.* **2004**, *104*, 1283.
- (22) Chen, P.; Xiong, Z.; Luo, J.; Lin, J.; Tan, K. L. *Nature* **2002**, *420*, 302.
- (23) Chen, P.; Xiong, Z.; Luo, J.; Lin, J.; Tan, K. L. *J. Phys. Chem. B* **2003**, *107*, 10967.
- (24) Hu, Y. H.; Yu, N. Y.; Ruckenstein, E. *Ind. Eng. Chem. Res.* **2005**, *44*, 4304.
- (25) Hu, Y. H.; Ruckenstein, E. *Ind. Eng. Chem. Res.* **2005**, *44*, 1510.
- (26) Hu, Y. H.; Yu, N. Y.; Ruckenstein, E. *Ind. Eng. Chem. Res.* **2004**, *43*, 4174.
- (27) Lu, J.; Fang, Z. Z. *J. Phys. Chem. B* **2005**, *109*, 20830.
- (28) Lu, J.; Fang, Z. Z.; Sohn, H. Y. presentation at MRS Spring Meeting 2006, San Francisco, CA, April 17–21, 2006.
- (29) Zaluski, L.; Zaluska, A.; Strom-Olsen, J. O. *J. Alloys Compd.* **1999**, *290*, 71.
- (30) Balema, V. P.; Pecharsky, V. K.; Dennis, K. W. *J. Alloys Compd.* **2000**, *313*, 69.
- (31) Balema, V. P.; Wiench, J. W.; Dennis, K. W.; Pruski, M.; Pecharsky, V. K. *J. Alloys Compd.* **2001**, *329*, 109.
- (32) Jang, J. W.; Shim, J. H.; Cho, Y. W.; Lee, B. J. *J. Alloys Compd.* In press paper, available online 5 December 2005.